Dalton Transactions

Accepted Manuscript

ROYAL SOCIETY OF CHEMISTRY

www.rsc.org/dalton

Two dimethylphenyl imidazole dicarboxylate-based lanthanide metal–organic frameworks for luminescence sensing of benzaldehyde†

Bingbing Shi, Yuanhao Zhong, Li Guo and Gang Li*

Two novel dimethylphenyl imidazole dicarboxylate-based lanthanide(III)-organic frameworks, $[Ln(H_2DMPhIDC)_3(H_3DMPhIDC)]_n$ (Ln = Eu (**1**), Tb (**2**); $H_3DMPhIDC$ = 2-(3,4-dimethylphenyl)-1*H*-imidazole-4,5-dicarboxylic acid) have been synthesized under hydrothermal conditions. Single crystal X-ray diffraction analyses reveal that polymers **1** and **2** crystallize in tetragonal space group $I4_1$, and exhibit isostructural three-dimensional (3D) solid-state frameworks. Both complexes indicate characteristic sharp emission bands of Eu^{3+} or Tb^{3+} ions, which are selectively sensitive to benzaldehyde-based derivatives (benzaldehyde, *m*-methylbenzaldehydes, *m*-carboxylbenzaldehyde and *m*-hydroxybenzaldehyde). These properties make both complexes potential fluorescence sensors for these chemicals.

Introduction

Over the past few years, luminescent lanthanide(III)- metal-organic frameworks (Ln-MOFs) have attracted much attention for their high thermal stability, strong emission, tunable colors and potential applications as luminescent materials, up-conversion emission, time-resolved microscopy, and so on.[1,2] Recently, a wide range of luminescent Ln-MOFs for sensing anions,[3] cations,[4,5] small molecules and high explosives[1b,6] have been realized. Considering the types of Eu^{3+} and Tb^{3+} MOFs showing characteristic, easily separable, line-like emission bands occurring in the green and red, respectively,[7] and having long-lived excited state life-times in the ms-range, they usually have been used to explore their sensing properties.[1b-1j, 3d, 4d,4e, 6d-6f]

Detection of small toxic organic molecules is a very important task for environmental protection and human health. Usually, benzaldehyde is mainly for the manufacture of lauryl aldehyde, lauric acid, light green, etc., and also can be used as solvent, plasticizer and low temperature lubricant, as a flavoring and fragrance in food, cosmetics, pharmaceuticals, and soap and for tobacco flavor. The presence of beyond the limits of benzaldehyde in food will not only seriously affect the people's health, but also can seriously pollute the environment.[8] In many

College of Chemistry and Molecular Engineering, Zhengzhou University, Zhengzhou 450001, Henan, P. R. China. E-mail: gangli@zzu.edu.cn

† Electronic supplementary information (ESI) available: The X-ray crystallographic files in CIF format. CCDC reference numbers 1009235 and 1009236 are for **1** and **2**, respectively.

countries, it is listed as one of the first control toxic chemicals.[8] Therefore, the development for the detection of benzaldehyde is critical in terms of environmental and safety considerations. So far, the official analytical methods to determine the quantity of benzaldehyde are based on the use of gravimetric and ultraviolet spectroscopic methods and polarographic analysis.[8] Luminescence quenching based chemical detection by using luminescent materials offers an alternative which is proven to be a much simpler, sensitive and convenient method,[9] it is mainly rely on the monitoring of transmission signals produced by the structural or electronic interaction between sensing materials and substrates. Nevertheless, to the best of our knowledge, reports about Ln-MOFs as luminescent probes for sensing benzaldehyde are not known.

Although several examples of imidazole dicarboxylate-based complexes as anion or cation sensors have been reported in the literature,[10-12] no related MOFs sensing of benzaldehyde have been described yet. Now, we are interest in investigating imidazole dicarboxylate-based Ln-MOFs with the goal to explore their applications for molecular recognition. Herein, we report two unique 3D isostructural luminescent MOFs, $[Ln(H_2DMPhIDC)_3(H_3DMPhIDC)]_n$ (Ln = Eu (**1**) and Tb (**2**), H_3DMPhIDC = 2-(3,4-dimethylphenyl)-1*H*-imidazole-4,5-dicarboxylic acid), which show high sensitivity and quick response toward the presence of trace amounts of benzaldehyde. Meanwhile, they can also detect trace amounts of benzaldehyde-based derivatives, such as *m*-methylbenzaldehyde, *m*-hydroxybenzaldehyde and *m*-carboxylbenzaldehyde. Such two MOFs may act as luminescent receptors for reversible and selective sensing for benzaldehydes. Further mechanism study will enlighten us to rational design and construct more luminescent MOFs materials for molecular sensing exploration.

Experimental section

Materials and methods

All chemicals were of reagent grade quality obtained from commercial sources and used without further purification. The organic ligand, H_3DMPhIDC was prepared according to the literature procedure.[13]

The C, H and N analyses were carried out on a FLASH EA 1112 analyzer. IR spectra were recorded on a BRUKER TENSOR 27 spectrophotometer as KBr pellets in the 400-4000 cm^{-1} region. TG measurements were performed by heating the crystalline samples from 20 to 850°C at

a rate of 10°C min^{-1} in air on a Netzsch STA 409PC differential thermal analyzer. X-ray powder diffraction (XRD) measurements were recorded on a Panalytical X'pert PRO X-ray diffractometer. Fluorescence spectra were characterized at room temperature by a F-4500 fluorescence spectrophotometer. The luminescent life time and quantum yield were determined on a FLsp920 full function steady/transient fluorescence spectrometer.

Preparation of crystalline polymer $[Eu(H_2DMPhIDC)_3(H_3DMPhIDC)]_n$ (1). A mixture of $Eu(NO_3)_3{\cdot}6H_2O$ (44.6 mg, 0.1 mmol), $H_3DMPhIDC$ (26.0 mg, 0.1 mmol), H_2O (7 mL) and oxalic acid (12.6 mg, 0.1 mmol) was sealed in a 25 mL Teflon-lined bomb and heated at 160 °C for 72 h. The reaction mixture was then allowed to cool to room temperature at a rate of 10 °C/h. The light-yellow rhombus crystals of **1** were collected, washed with distilled water, and dried in air (70% yield based on Eu). Anal. Calcd for $C_{52}H_{45}N_8O_{16}Eu$: C, 52.44; H, 3.78; N, 9.41%. Found: C, 52.62; H, 3.56; N, 9.03%. IR (cm^{-1}, KBr): 3446 (m), 3154 (m), 2919 (w), 1633 (w), 1549 (s), 1489 (w), 1403 (s), 1383 (s), 1268 (w), 1286 (m), 1260 (m), 1128 (s), 1021 (w), 823 (s), 733 (m), 561 (m), 533 (w), 517 (w), 440 (m).

Preparation of crystalline polymer $[Tb(H_2DMPhIDC)_3(H_3DMPhIDC)]_n$ (2). Polymer **2** was prepared in a manner analogous to that used to prepare **1** only $Tb(NO_3)_3{\cdot}6H_2O$ (45.3 mg, 0.1 mmol) was used instead of $Eu(NO_3)_3{\cdot}6H_2O$. The light-yellow rhombus crystals of **2** were collected, washed with distilled water, and dried in air (65% yield based on Tb). Anal. Calcd for $C_{52}H_{45}N_8O_{16}Tb$: C, 52.14; H, 3.76; N, 9.36%. Found: C, 52.36; H, 3.98; N, 9.13%. IR (cm^{-1}, KBr): 3446 (m), 3173 (m), 2946 (w), 2919 (m), 1704 (w), 1548 (s), 1493 (m), 1403 (s), 1381 (s), 1287 (w), 1260 (m), 1223 (m), 1106 (s), 1021 (w), 879 (s), 823 (s), 733 (s), 559 (m), 533 (w), 516 (w), 438 (m).

Luminescence measurements. The luminescence properties of **1** and **2** were investigated in solid state and in various solvent emulsions at room temperature. The **1** (or **2**) –solvent emulsions were prepared by introducing 3 mg of **1** (or **2**) crystalline powder into 3.0 mL of different organic solvents, including alcohols (methanol, ethanol, and *n*-butyl alcohol), ketones (acetone), ethers (THF), amides (DMF), acetonitrile, chloroalkanes (CH_2Cl_2, $CHCl_3$), aldehydes (methanal, glyoxal) and so on, and treated by ultrasonication for 30 min, and then formed stable suspensions

for fluorescence study. For sensing properties with respect to benzaldehyde, different amounts of benzaldehyde were introduced into a **1** (or **2**) emulsion in acetone solution. The related sensing properties of **1** (or **2**) to liquid 3-methylbenzaldehyde were determined by the similar procedure as benzaldehyde. The two solid chemicals, *m*-hydroxybenzaldehyde (3.5 g) or *m*-carboxybenzaldehyde (1.5 g), were dissolved in 3 ml of DMF, respectively. Then the finely ground samples of **1** or **2** (3 mg) were dispersed in the above DMF solution, treated by ultrasonication to form stable suspensions for luminescent quenching experiment.

The experimental details of quenching and recovery cycles of **1** and **2** are as follows: The air dried **1** (3 mg) was added to a solution of acetone (3 mL) and the emission spectrum without the addition of benzaldehyde was recorded. Then the samples were separated from the acetone by centrifuging, and dispersed into solution of benzaldehyde (3.0 mL), and treated by ultrasonication for 30 min forming stable suspensions for fluorescence quenching study. After then, the resulting suspension was transferred to a centrifuge tube. After being repeatedly washed by acetone and centrifuged for three times, the material was air dried for another cyclic test.

Crystal structure determinations. Suitable single crystals of compounds **1** and **2** were selected for single-crystal X-ray diffraction analyses. The intensity data were measured on a Bruker Smart 1000 diffractometer with a graphite-monochromated Mo-Kα radiation (λ = 0.71073 Å). Single crystals of **1** and **2** were selected and mounted on a glass fiber. All data were collected at room temperature using the ω-2θ scan technique and corrected for Lorenz-polarization effects. A correction for secondary extinction was applied.

The two structures were solved by direct methods and expanded using the Fourier technique. The non-hydrogen atoms were refined with anisotropic thermal parameters. The hydrogen atoms on C were positioned geometrically and refined using a riding model. The hydrogen atoms on O were found at reasonable positions in the differential Fourier map and located there. All the hydrogen atoms were included in the final refinement. The final cycle of full-matrix least squares refinement was based on 5330 observed reflections and 367 variable parameters for **1**, 5425 observed reflections and 370 variable parameters for **2**. All calculations were performed using the SHELX-97 crystallographic software package.[14] The crystallographic data and selected bond lengths and angles are given in Tables 1 and 2, respectively.

Although the Platon program implied that $I4_1/a$ was the right space group, we were not able to

refine the structures in $I4_1/a$ with low R factors. The final R factors are about 17% for both structures in space group $I4_1/a$. By reexamine again the two disordered sites of metal ion in $I4_2$, i.e. Tb1 and Tb2, their refined SOFs are 0.73 and 0.27, respectively. That means although the organic parts possess the symmetry of $I4_1/a$, the disordered metal ions do not. So we think $I4_1$ is the right choice for these isostructural series. To have reasonable bond distances and angles for O-H and N-H, we have used some restraints (please see the CIF files).

Results and discussion

Crystal structures of crystalline polymers $[Ln(H_2DMPhIDC)_3(H_3DMPhIDC)]_n$ (Ln = Eu (1) and Tb (2)

Since Ln-MOFs **1** and **2** are isostructural, the single crystal structure of 1 is only analyzed here. Polymer **1** crystallizes in tetragonal space group $I4_1$. The asymmetric unit of **1** is composed of one crystallographically distinct Eu^{3+} center, three $H_2DMPhIDC^-$ and one $H_3DMPhIDC$ ligands. As shown in Fig. 1a, the $Eu1^{3+}$ ion is octacoordinated with six oxygen atoms (O1, O1c, O4e, O4d, O8 and O8c) and two nitrogen atoms (N1 and N1c) from the carboxylate groups of four different $H_2DMPhID^-$ ligands (Eu-O distances ranging from 2.35(1) to 2.79(1) Å). The $Eu2^{3+}$ ion is six-coordinated with six oxygen atoms (O4e, O4d, O5d, O5f, O8 and O8c) from the carboxylate groups of four organic ligands. The Eu-L (L = N or O) distances are in the range of 2.35(1)-2.93(1) Å and the trans L-Eu-L bond angles vary from 66.2(2) to 158.1(2)°, all of which are comparable to those reported values of Eu^{3+} complexes.[15] The $H_2DMPhIDC^-$ and $H_3DMPhIDC$ units in **1** adopt two different coordination modes, μ_3-*k*O:*k*O′,N, and μ_3-*k*O:*k*O:*k*O′ mode, respectively (Scheme 1).

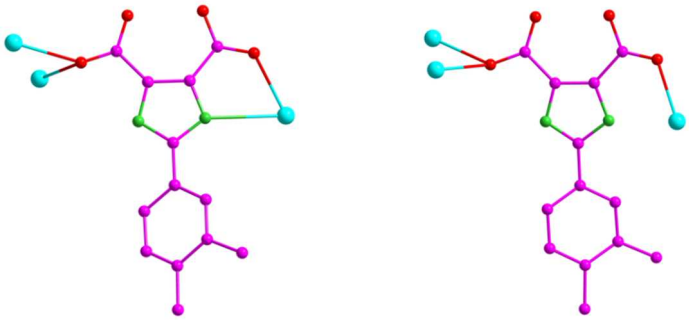

Scheme 1 Coordination modes of the imidazole dicarboxylate ligands

In **1**, Eu1 and Eu2 atoms are bridged by four symmetry-related $H_2DMPhID^-$ ligands in mode μ_3-*k*O:*k*O:*k*O′ (Scheme 1b) to generate a dinuclear Eu^{3+} secondary building unit (SBU) with the Eu···O and Eu···Eu distances being 2.33-2.76 and 2.79 Å, respectively. Consequently, the dinuclear units are connected to four adjacent ones through two organic ligands in bridging modes (Scheme 1), leading to a 3D solid-state structure (Fig. 1b).

To understand the intricate framework better, we achieved by the application of a topological approach, reducing multidimensional structure to simple nodes and connection nets. Each imidazole dicarboxylate ligand connects two dinuclear Eu^{3+} SBUs acting as a 2-connected node, while each dinuclear cluster unit bridges four imidazole dicarboxylate ligands as a four-connected node. Thus, **1** can be considered as a (2,4)-connected network with the point symbol of 6^6 (Fig. 1c).

It is worth noting that in the preparation process of **1** and **2**, we originally hoped to introduce oxalic acid to the reaction system as a coligand, but to our surprise, the oxalic acid ligand does not coordinate to the metal ion and a new 3D polymer only containing $H_3DMPhIDC$ ligand was obtained. If the reaction was performed without oxalic acid, no any suitable crystals produced. We guess that the oxalic acid may act as template agent for the construction of novel MOFs.

XRD patterns and thermal analyses

To confirm the phase purity of the two polymers, the XRD patterns were recorded. Most of the peak positions of simulated and experimental patterns are in good agreement with each other (Figures S1 and S2, see the supporting information).

The TG curves have been obtained under flowing air for crystalline samples of **1** and **2** in the temperature range 20−850°C (Figure 7).

The TG curve indicates that **1** exhibits an initial mass loss of 66.22% (calculated 65.30%) corresponding to the dissociation of the parts of the imidazole dicarboxylate ligands, and then reveals a weight loss of 15.93% (calculated 19.83%) from 422.5 to 612.5°C for the removal of remaining organic units of the imidazole dicarboxylate ligands. Finally, a plateau region is observed from 612.5°C to 847.5°C, the remaining weight of 17.85% is attributed to the percentage (calculated 14.80%) of the Eu and O components, indicating that the final product is $0.5Eu_2O_3$.

For polymer **2**, the initial weight loss corresponding to the release of three imidazole dicarboxylates is observed from 47.0 to 425.0°C (observed 63.41%, calculated 64.97%), and then reveals a weight loss of 22.20% (calculated 21.66%) from 425.0 to 667.0°C for the removal of the remaining parts of the imidazole dicarboxylate ligands. A plateau region from 667.0 to 847.0°C appeared. The amorphous residue of $0.5Tb_2O_3$ (observed 14.39%, calculated 13.37%) is remained.

In conclusion, the thermal data of the polymers are in reasonable agreement with the crystal structure analyses.

Luminescence behaviors and sensing properties

Ln-MOFs have received much attention due to their potential applications in molecular sensors, as probes in biomedical assays, in electroluminescent displays and so on.[1,6,16] Inspired by such interesting luminescent properties of the Ln-MOFs, the solid-state fluorescent and sensing properties of **1** and **2** have been investigated at room temperature.

The luminescent spectrum of the free ligand H_3DMPhIDC can be found in the literature, [17] which exhibits an emission peak at 394 nm with an excitation wavelength of 346 nm, which may be attributed to ligand-centered $\pi^* \rightarrow n$ electronic transitions.

It can be seen from Fig. S3a and S3b, polymers **1** and **2** show characteristic emission of lanthanide ions. Polymer **1** exhibits characteristic transitions of Eu^{3+} ion at 591 and 616 nm, which correspond to $^5D_0 \rightarrow {}^7F_1$ and $^5D_0 \rightarrow {}^7F_2$ transitions, respectively (λex = 345 nm) (Fig. S3a). Polymer **2** indicates four peaks at 490, 547, 586, and 622 nm corresponding to $^5D_4$-$^7F_6$, $^5D_4$-$^7F_5$, $^5D_4$-$^7F_4$ and $^5D_4$-$^7F_3$ transitions, respectively, of Tb^{3+} ion (Fig. S3b). The emission band $^5D_4$-$^7F_5$ is distinctly stronger than the other mission bands $^5D_4$-$^7F_6$, $^5D_4$-$^7F_4$ and $^5D_4$-$^7F_3$. It is in agreement with the characteristic emission of Tb^{3+} ion in related Tb^{3+} complexes[18]. For the two complexes, the $^5D_0 \rightarrow {}^7F_2$ and $^5D_4 \rightarrow {}^7F_5$ transitions are the strong ones, showing higher color purity and emission intensity, which are extremely sensitive to the chemical environment around the Eu^{3+} or Tb^{3+} ions.[1c] This clearly demonstrates that the organic imidazole dicarboxylate ligand, H_3DMPhIDC is a good sensitizer for Eu^{3+} or Tb^{3+} luminescent emission in our polymeric systems.

To explore the potential applications of the polymers for probing small molecules, we firstly

determined the solvent effect on the luminescent properties of **1** and **2**. The finely ground samples of **1** (or **2**) (3 mg) was dispersed in 3 mL of different solvents, including, water, alcohols (methanol, ethanol, and *n*-butyl alcohol), ketones (acetone), ethers (THF), amides (DMF), acetonitrile, chloroalkanes (CH_2Cl_2, $CHCl_3$), aldehydes (methanal, glyoxal) and even other aromatic complexes (benzene, methylbenzene, benzaldehyde), treated by ultrasonication for 30 min forming stable suspensions for fluorescence studies. As shown in Fig. 2, the luminescent intensity of $^5D_0 \rightarrow {}^7F_2$ transition for Eu^{3+} ion or of $^5D_4 \rightarrow {}^7F_5$ transition for Tb^{3+} ion in the suspensions heavily depends on the type of solvent: For **1**: several solvents, water, acetone, CH_2Cl_2, $CHCl_3$, and methanol have basically no effect on the Eu-luminescence, while other solvents, DMF, THF, methanal, acetonitrile, *n*-butyl alcohol and benzene have varying degrees of quenching effects on the luminescent intensity. The luminescent intensity is about half of the water one after dispersed in benzene or methylbenzene. Inpressively, there is almost no characteristic emission of Eu^{3+} ion for benzaldehyde. For **2**, there is still almost no characteristic emission of Tb^{3+} ion for benzaldehyde. Compared with other solvents, **1** (or **2**) indicates a selective response to benzaldehyde molecule.

To examine the sensing sensitivity towards benzaldehyde in more detail, a batch of suspensions of compounds **1** or **2** in acetone solution with gradually increasing benzaldehyde contents were prepared, and their emission spectra were recorded (Because polymers **1** or **2** dispersed in acetone solvent shows same emission spectra as their solid-state samples, acetone was utilized as dispersion medium). As shown in Fig. 3, it can be clearly seen that the fluorescence intensity gradually decrease with increase of benzaldehyde content, which indicates that **1** (or **2**) is a promising fluorescent probe for detecting benzaldehyde.

In addition, we investigated the fluorescent quenching properties of other aromatic aldehydes (*m*-methylbenzaldehydes, *m*-carboxylbenzaldehyde, and *m*-hydroxybenzaldehyde). The emission spectra (Fig. 4) show that the three aromatic aldehydes can also efficiently quench the fluorescence. For **1**, benzaldehyde quenches the luminescent intensity most significantly (benzaldehyde 98.97%, *m*-carboxylbenzaldehyde 98.81%, *m*-hydroxybenzaldehyde 97.70%, *m*-methylbenzaldehydes 98.57%). *m*-Methylbenzaldehyde significantly quenches the emission intensity for **2** (benzaldehyde 99.78%, *m*-carboxylbenzaldehyde 99.80%, *m*-hydroxybenzaldehyde 99.85%, *m*-methylbenzaldehyde 99.94%). It is clear that **1**- and **2**-solvents show different degree of fluorescent intensity decrease, while the fluorescence

quenching response of **2** is more obvious. The results demonstrate the ability of **1** and **2** as a fluorescence sensor to detect the aromatic aldehydes. As shown in Fig. S4, with increasing of *m*-methylbenzaldehyde content, the emission intensity of **1**- or **2**-*m*-methylbenzaldehyde-acetone also decreases gradually, which indicate **1** and **2** are also promising fluorescent probes for detecting these chemicals.

Luminescence lifetimes of complexes **1** and **2** were investigated in solid state. The luminescent decay and fitted curves (not shown), with emission monitored at $^5D_0 \rightarrow {}^7F_2$ for Eu^{3+} and $^5D_4 \rightarrow {}^7F_5$ for Tb^{3+}, respectively, were adjusted with a bi-exponential function. The lifetime (τ) of 771 μs (χ^2 = 1.096) for **1** and 1065 μs (χ^2 = 1.238) for **2**. By comparing the values obtained for the original samples of the complexes with the solid samples obtained by centrifugal separation from benzaldehyde solvent, the lifetimes show little change. As for quantum efficiency, there is almost no change for **1** (or **2**) before and after dispersing in benzaldehyde (η = 0.05 for **1**; η = 0.71 for **2**). The measurements reveal that **2** shows longer luminescence lifetime and higher quantum efficiency than those for **1**. It is worth mentioning that the photoluminescence quantum efficiency of **2** is a large value compared with other terbium complexes,[18] which may also make polymer **2** a good candidate for photoactive material.

To date, the mechanism for such quenching effects of small solvent molecules is still not very clear.[6f] To elucidate the possible mechanism for such luminescence diminishment by various organic solvents as well as to identify if the frameworks of **1** and **2** collapse in different solvents, solid samples were obtained by centrifugal separation from the organic solvents. The XRD spectra of the as-synthesized products are in good agreement with the corresponding simulated ones, indicating the phase purities of the samples. In addition, XRD data showed that there was almost no difference in **1** (or **2**) immersing in different solvents before or after, indicating that the original framework remains unchanged upon solvent treatment. So, the introduction of various solvents on the surface of **1** or **2**, in our opinion, hardly affects their structures. As representative examples, XRD patterns for the complexes after immersion in ethanol or benzaldehyde are presented in Figs. S1 and S2.

It is well-known that the efficient lanthanoid luminescence in organometallic complexes is typically depends on the efficiency of the energy transfer from the ligand to Ln^{3+} center.[19] As stated above, due to the fact that polymers **1** and **2** are isomorphic, only the compound **1** has been analyzed. The antenna-effect in the MOF of **1** is induced by the energy transfer from the

imidazole dicarboxylate ligands to Eu^{3+} and results in the strong luminescence of **1**. Upon addition of benzaldehyde, close contact may occur between **1** and benzaldehyde. It is most likely that the antenna-effect in **1** is weakened by benzaldehyde though O–H···O hydrogen bonds between the imidazole dicarboxylate ligands and benzaldehyde molecules. That is to say, this may lead to the energy transformation from the imidazole dicarboxylate ligands to benzaldehyde, and thus reduce the ligand−metal energy transformation (LMET) efficiency, leading to the quenching effect on the luminescent intensity (Fig. 5), which may be similar with ionic sensing through hydrogen bonding interactions.[20] Because the other related benzaldehyde derivatives show similar luminescent quenching effects for **1** or **2**, we think the quenching mechanism is similar. However, the specific cause of the remarkably different quenching effects of various solvents is unknown, and the mechanism for such quenching effects still remains to be further studied.

The sensing ability of **1** could be regenerated and reused even after several cycles of sequential alternative addition of acetone and benzaldehyde. The luminescent intensity of **1** in acetone after five cycles of quenching and recovery does not decrease compared with the initial state. These results indicate that this compound possesses high stability for its repeated usage in benzaldehyde detection application and can be an excellent candidate as a benzaldehyde sensor. The similar experiments show that **2** also has similar good recovery properties.

Conclusion

In summary, two novel luminescent 3D Eu-MOF and Tb-MOF based on semi-rigid ligand H_3DMPhIDC has been successfully synthesized under hydrothermal conditions. The selectivity and sensitivity of the fluorescence response of **1** and **2** to benzaldehyde show that they could be used as efficient fluorescence sensors for benzaldehyde. Moreover, complexes **1** and **2** can also detect the derivatives of benzaldehyde. Further study and speculation of the mechanism illustrate that the majority of the luminescent response to solvent molecules can result from the interaction of substrate (like benzaldehyde, *m*-methylbenzaldehydes, *m*-carboxylbenzaldehyde, or *m*-hydroxybenzaldehyde) with the imidazole dicarboxylate ligands, and thus affect the LMET efficiency, and consequently lead to luminescent quenching effects. The luminescent mechanism will inspire us to construct more luminescent Ln-MOFs to explore their sensing properties. This

study extends the applications of imidazole dicarboxylate-based Ln-MOFs as chemosensors for small molecules.

Acknowledgments

We gratefully acknowledge the financial support by the National Natural Science Foundation of China (21341002 and J1210060), and the Natural Science Foundation of Henan Education Department (13A150655).

References

(1) (a) Z. Jin, H. M. He, H. Y. Zhao, T. Borjigin, F. X. Sun, D. M. Zhang, G. S. Zhu, *Dalton Trans*., 2013, **42**, 13335; (b) Y. Chen, S. Q. Ma, *Rev. Inorg. Chem*., 2012, 32, 81. (c) Z. C. Hu, B. J. Deibert, J. Li, *Chem. Soc. Rev*., 2014, **43**, 5815; (d) Y. J. Cui, B. L.Chen, G. D.Qian, *Coord. Chem. Rev*. 2014, **273**, 76. (e) M. D. Allendorf, C. A. Bauer, R. K. Bhakta, R. J. T. Houk, *Chem. Soc. Rev*., 2009, **38**, 1330. (f) Y. J. Cui, Y. F. Yue, G. D. Qian and B. L. Chen, *Chem. Rev*. 2012, **112**, 1126. (g) L. E. Kreno, K. Leong, O. K. Farha, M. Allendorf, R. P. V. Duyne and J. T. Hupp, *Chem. Rev*. 2012, **112**, 1105. (h) M. D. Allendorf, C. A. Bauer, R. K. Bhaktaa and R. J. T. Houka, *Chem. Soc. Rev*. 2009, **38**, 1330. (i) S. Roy, A. Chakraborty, T. K. Maji, *Coord. Chem. Rev*. 2014, **273**,139. (j) Q.-L. Zhu, Q. Xu, *Chem. Soc. Rev*., 2014, **43**, 5468.

(2) (a) B. L. Chen, L. B. Wang, Y. Q. Xiao, F. R. Fronczek, M. Xue, Y. J. Cui, G. D. Cui, *Angew. Chem., Int. Ed*., 2009, **48**, 500; (b) H. L. Jiang, Q. Xu, *Chem. Commun*., 2011, **47**, 3351; (c) H. L. Jiang, N. Tsumori, Q. Xu, *Inorg. Chem*., 2010, **49**, 10001.

(3) (a) C. A. Bauer, T. V. Timofeeva, T. B. Settersten, B. D. Patterson, V. H. Liu, B. A. Simmons, M. D. Allendorf, *J. Am. Chem. Soc*., 2007, **129**, 7136; (b) B. L. Chen, L. B. Wang, F. Zapata, G. D. Qian, E. B. Lobkovsky, *J. Am. Chem. Soc.*, 2008, **130**, 6718; (c) M. Montalti, L. Prodi, N. Zaccheroni, L. Charbonniere, L. Douce, R. Ziessel, *J. Am. Chem. Soc.*, 2001, **123**, 12694. (d) X. H. Wang, H. J. Chang, J. Xie, B.Z. Zhao, B.T. Liu, S.L. Xu, W.B. Pei, N. Ren, L.Huang, W. Huang, *Coord. Chem. Rev*. 2014, **273**, 201.

(4) (a) N. A. J. Sommerdijk, A. Poppe, C. A. Gibson, J. D. Wright, *J. Mater. Chem*., 1998, **8**, 565; (b) B. L. Chen, L. B. Wang, Y. Q. Xiao, F. R. Fronczek, M. Xue, Y. J. Cui, G. D. Qian, *Angew. Chem., Int. Ed*., 2009, 4**8**, 500; (c) Y. W. Li, J. R. Li, L. F. Wang, B. Y. Zhou, Q. Chen, X. H. Bu, *J. Mater. Chem. A,* 2013, **1**, 495. (d) W. Liu, T. Jiao, Y. Li, Q. Liu, M. Tan, H. Wang and L. Wang, *J. Am. Chem. Soc.*, 2004, **126**, 2280. (e) B. Liu, W. P. Wu, L . Hou, Y. Y. Wang, *Chem. Commun*. 2014, **50**, 8731.

(5) (a) W. T. Yang, J. Feng, H. J. Zhang, *J. Mater. Chem*., 2012, **22**, 6819; (b) H. M. Wang, Y. Y. Yang, C. H. Zeng, T. S. Chu, Y. M. Zhu, S. W. Ng, *Photochem. Photobiol. Sci*., 2013, **12,** 1700.

(6) (a) J. Zhao, H. M. He, H. Y. Zhao, T. Borjigin, F. X. Sun, D. M. Zhang, G. S. Zhu, *Dalton Trans*., 2013, **42**, 13335; (b) D. Y. Ma, W. X. Wang, Y. W. Li, J. Li, C. G. Calvez, O. Guillou, *CrystEngComm*, 2010, **12**, 4372; (c) D. Tian, Y. Li, R. Y. Chen, Z. Chang, G. Y. Wang, X. H. Bu, *J. Mater. Chem. A*, 2014, **2**, 1465. (d) B. Chen, Y. Yang, F. Zapata, G. Lin, G. Qian and E. B. Lobkovsky, *Adv. Mater*., 2007, **19**, 1693. (e) Q. B. Bo, H. T. Zhang, H. Y. Wang, J. L. Miao, Z. W. Zhang, *Chem. A Eur. J*., 2014, **20**, 3712. (f) J. M. Zhou, W. Shi, H. M. Li, H. Li, P. Cheng, *J. Phys. Chem. C*, 2014, **118**, 416 and references therein.

(7) (a) D. L. Long, A. J. Blake, N. R. Champness, C. Wilson, M. Schroeder, *J. Am. Chem. Soc*., 2001, **123**, 3401; (b) D. Parker, *Chem.Soc. Rev*., 2004, **33**, 156; (c) J. Rocha, L. D. Carlos, F. A. A. Paz, D. Ananias, *Chem. Soc. Rev*., 2011, **40**, 926.

(8) (a) AOAC International, Official Methods of Analysis of AOAC International, Chapter 36, 1995, 18. (b) V. J. Koshy, J. V. Prasad, G. Kalpana, S. Satish, *Anal. Chim. Acta*, 1995, **307**, 55; (c) L. H. Wang, Z. S. Chen, *Electroanalysis*, 1996, **8**, 842; (d) M. B. Sanz, L. A. Sarabia, A. Herrero, M. C. Ortiz, *Talanta*, 2002, **56**, 1039.

(9) (a) S. Pramanik, C. Zheng, X. Zhang, T. J. Emge, J. Li, *J. Am. Chem. Soc*., 2011, **133**, 4153; (b) Z. Chen, Y. W. Sun, L. L. Zhang, D. Sun, F. L. Liu, Q. G. Meng, R. M. Wang, D. F. Sun, *Chem. Commun*., 2013, **49**, 11557; (c) A. Balamurugan, V. Kumar, M. Jayakannan, *Chem. Commun*., 2014, **50**, 842; (d) B. Gole, A. K. Bar, P. S. Mukherjee, *Chem. Commun*., 2011, **47**, 12137.

(10) Y. H. Zheng, C. L. Tan, Q. M. Wang and C. C. Zhang, *Solid State Sci*. 2011, **13**, 1687.

(11) S. Das, D. Saha, C. Bhaumik, S. Dutta and S. Baitalik, *Dalton Trans*. 2010, **39**, 17.

(12) (a) S. L. Cai,; S. R. Zheng, J. Fan, T. T. Xiao, J. B. Tan and W. G. Zhang, *Inorg. Chem. Commun*. 2011, **14**, 937; (b) Z. F. Yue, Z. N. Chen, M. J. Yao, H. L. Wang, G. Li, *RSC Adv*. 2014, **4**, 33537.

(13) (a) H. K. Fun, S. S. S. Raj, R. G. Xiong, J. L. Zuo, Z. Yu, X. Z. You, *J. Chem. Soc., Dalton Trans*., 1999, 1915; (b) M. R. Grimmett, Product class 3: imidazoles. *Org. Chem.* 2002, **12**, 325.

(14) G. M. Shelddrick, SHELX-97, Program for the Solution and Refinement of Crystal Structures, University of Göttingen, Germany 1997.

(15) (a)W. G. Lu, L. Jiang, X. L. Feng, T. B. Lu, *Inorg. Chem*., 2009, **48**, 6997; (b) P. Mahata, K. V. Ramya, S. Natarajan, *Dalton Trans*., 2007, 4017; (c) W. T. Chen, S. Fukuzumi, *Inorg. Chem*., 2009, **48**, 3800; (d) W. G. Lu, L. Jiang, T. B. Lu, *Cryst. Growth Des*., 2010, **10**, 4310.

(16) K. L. Wong, G. L. Law, Y. Y. Yang, W. T. Wong, *Adv. Mater*., 2006, **18**, 1051.

(17) (a) C. J. Wang, T. Wang, W. Zhang, H. J. Lu, G. Li, *Cryst. Growth Des*., 2012, **12**, 1091; (b) C. J. Wang, T. Wang, L. Li, B. B. Guo, Y. Zhang, Z. F. Xiong, G. Li, *Dalton Trans.*, 2013, **42**, 1715.

(18) M. D. Allendorf, C. A. Bauer, R. K. Bhakta, R. J. T. Houk, *Chem. Soc. Rev*., 2009, **38**, 1330.

(19) N. Arnaud, E. Vaquer, J. Georges, *Analyst*, 1998, **123**, 261.

(20) (a) G. L. Law, T. A. Pham, J. D. Xu, K. N. Raymond, *Angew. Chem., Int. Ed*., 2012, **51**, 2371; (b) C. H. Zeng, J. L. Wang, Y. Y. Yang, T. S. Chu, S. L. Zhong, W. T. Wong, *J. Mater. Chem. C,* 2014, **2**, 2235. (c) B.

Chen, L. Wang, F. Zapata, G. Qian, E. B. Lobkovsky, *J. Am. Chem. Soc*., 2008, **130**, 6718.

Table 1. Crystallographic data for compounds **1** and **2**

	1	**2**
Formula	$C_{52}H_{45}N_8O_{16}Eu$	$C_{52}H_{45}N_8O_{16}Tb$
Formula weight	1189.91	1196.88
Crystal system	tetragonal	tetragonal
Space group	$I4_1$	$I4_1$
Crystal size	0.28 × 0.27 × 0.24	0.28 × 0.27 × 0.21
a (Å)	16.688(7)	16.614(4)
b (Å)	16.688(7)	16.614(4)
c (Å)	17.360(14)	17.335(10)
α (deg)	90	90
β (deg)	90	90
γ (deg)	90	90
V (Å^3)	4835(5)	4784.9(3)
Z	4	4
Dc (mg m^{-3})	1.633	1.661
F(000)	2412	2424
μ (mm^{-1})	1.382	1.563
Reflns collected unique	13597 /5330 R(int) = 0.0611	15389 / 5425 R(int) = 0.0340
Data/restraints/parameters	5330 / 4 / 367	5425 / 4 / 370
Goodness-of-fit on F^2	1.021	1.009
Final R indices [a] [$I > 2\sigma$(I)]	R_1 = 0.0482; wR_2 = 0.1226	R_1 = 0.0316; wR_2 = 0.0723
R indices (all data)	R_1 = 0.0696; wR_2 = 0.1442	R_1 = 0.0420; wR_2 = 0.0755

[a] $R_1 = \Sigma[|Fo|-|Fc|]/\Sigma|Fo|$ $\quad wR_2 = [\Sigma(|Fo|-|Fc|)^2 / \Sigma|Fo|^2]^{1/2}$

Table 2. Selected bond distances (Å) and angles (deg) for complexes **1** and **2**

1					
Eu(1)-O(4)#1	2.35(1)	Eu(1)-O(4)#2	2.35(1)	Eu(1)-O(8)	2.36(1)
Eu(1)-O(1)	2.41(1)	Eu(1)-O(1)#3	2.41(1)	Eu(1)-N(1)	2.82(1)
Eu(1)-N(1)#3	2.82(1)	Eu(2)-O(8)	2.47(1)	Eu(2)-O(8)#3	2.47(1)
Eu(2)-O(5)#4	2.51(1)	Eu(2)-O(4)#1	2.79(1)	Eu(2)-N(3)#5	2.93(1)
O(4)#1-Eu(1)-O(4)#2	130.0(3)	O(4)#1-Eu(1)-O(8)	77.6(2)	O(4)#2-Eu(1)-O(8)	75.5(2)
O(4)#2-Eu(1)-O(8)#3	77.6(2)	O(8)-Eu(1)-O(8)#3	113.4(3)	O(4)#1-Eu(1)-O(1)	146.2(2)
O(4)#2-Eu(1)-O(1)	75.4(2)	O(8)-Eu(1)-O(1)	135.5(2)	O(8)#3-Eu(1)-O(1)	92.2(2)
O(4)#2-Eu(1)-O(1)#3	146.2(2)	O(8)-Eu(1)-O(1)#3	92.2(2)	O(1)-Eu(1)-O(1)#3	93.6(3)
O(4)#1-Eu(1)-Eu(2)	65.0(2)	O(8)-Eu(1)-Eu(2)	56.7(2)	O(4)#1-Eu(1)-N(1)	83.3(2)
O(4)#2-Eu(1)-N(1)	125.8(2)	O(8)-Eu(1)-N(1)	158.1(2)	O(8)#3-Eu(1)-N(1)	71.3(2)
O(8)-Eu(2)-O(8)#3	105.8(3)	O(8)-Eu(2)-O(5)#4	87.9(2)	O(8)-Eu(2)-O(5)#5	154.4(2)
O(5)#4-Eu(2)-O(5)#5	88.5(4)	O(8)-Eu(2)-O(4)#2	66.2(2)	O(5)#4-Eu(2)-O(4)#2	99.4(2)
2					
Tb(1)-O(4)#1	2.34(1)	Tb(1)-O(4)#2	2.338(3)	Tb(1)-O(8)	2.35(1)
Tb(1)-O(1)	2.39(1)	Tb(1)-N(1)	2.831(3)	Tb(2)-O(5)#4	2.43(1)
Tb(2)-O(8)	2.45(1)	Tb(2)-O(4)#2	2.758(4)	Tb(2)-N(3)#5	2.93(1)
O(4)#1-Tb(1)-O(4)#2	128.9(2)	O(4)#1-Tb(1)-O(8)	76.83(13)	O(4)#2-Tb(1)-O(8)	75.4(1)
O(4)#2-Tb(1)-O(8)#3	76.8(1)	O(8)-Tb(1)-O(8)#3	112.44(19)	O(4)#1-Tb(1)-O(1)	146.2(1)
O(4)#2-Tb(1)-O(1)	76.3(1)	O(8)-Tb(1)-O(1)	136.34(11)	O(8)#3-Tb(1)-O(1)	92.4(1)
O(4)#1-Tb(1)-O(1)#3	76.3(1)	O(1)-Tb(1)-O(1)#3	92.98(16)	O(4)#1-Tb(1)-Tb(2)	64.4(1)
O(8)-Tb(1)-Tb(2)	56.22(9)	O(1)-Tb(1)-Tb(2)	133.51(8)	O(4)#1-Tb(1)-N(1)	83.6(1)
O(4)#2-Tb(1)-N(1)	126.11(10)	O(1)-Tb(1)-N(1)	62.55(9)	O(5)#4-Tb(2)-O(5)#5	87.4(3)

Symmetry transformations	O(5)#4-Tb(2)-O(8)	88.5(2)	O(5)#5-Tb(2)-O(8)	154.2(1)	O(8)-Tb(2)-O(8)#3	105.5(2
	O(5)#4-Tb(2)-O(4)#2	100.0(1)	O(5)#5-Tb(2)-O(4)#2	139.3(1)	O(8)-Tb(2)-O(4)#2	66.4(1)
	O(5)#4-Tb(2)-O(4)#1	139.3(1)	O(5)#5-Tb(2)-O(4)#1	100.0(1)	O(8)#3-Tb(2)-O(4)#1	66.4(1)

used to generate equivalent atoms for **1**: #1: y-1/2, -x+1, z-1/4. #2: -y+3/2, x, z-1/4. #3: -x+1, -y+1, z. #4: y+1/2, -x+1, z-1/4. #5: -y+1/2, x, z-1/4. For **2**: #1: y-1/2, -x+1, z-1/4. #2: -y+3/2, x, z-1/4. #3: -x+1, -y+1, z. #4: y+1/2, -x+1, z-1/4. #5: -y+1/2, x, z-1/4.

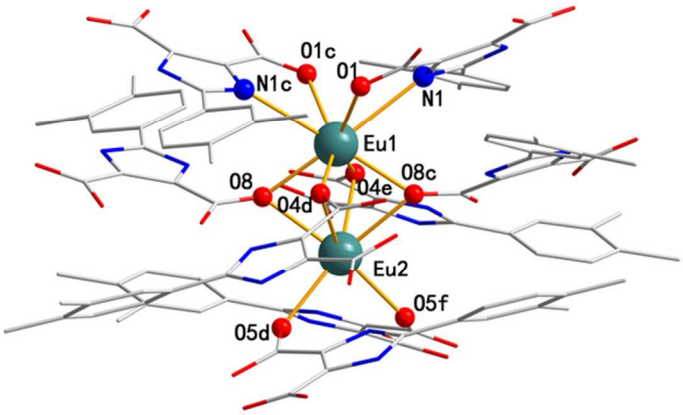

(a)

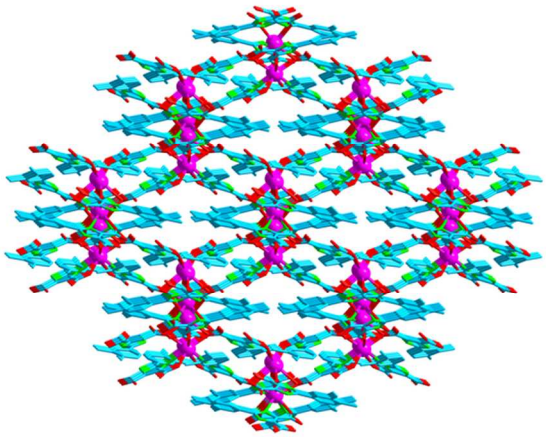

(b)

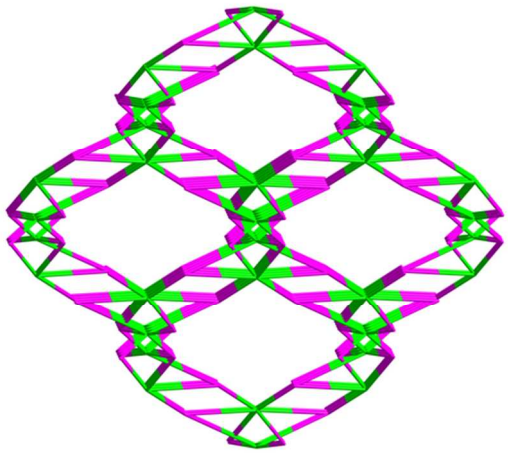

(c)

Figure 1. (a) Coordination environments of Eu^{3+} atoms in **1** (H atoms omitted for clarity). (b) Schematic view of the 3D framework of **1**. (c) The (2,4)-connected network of **1** by considering the ligand as a 2-connected node and Eu^{3+} as a 4-connected node.

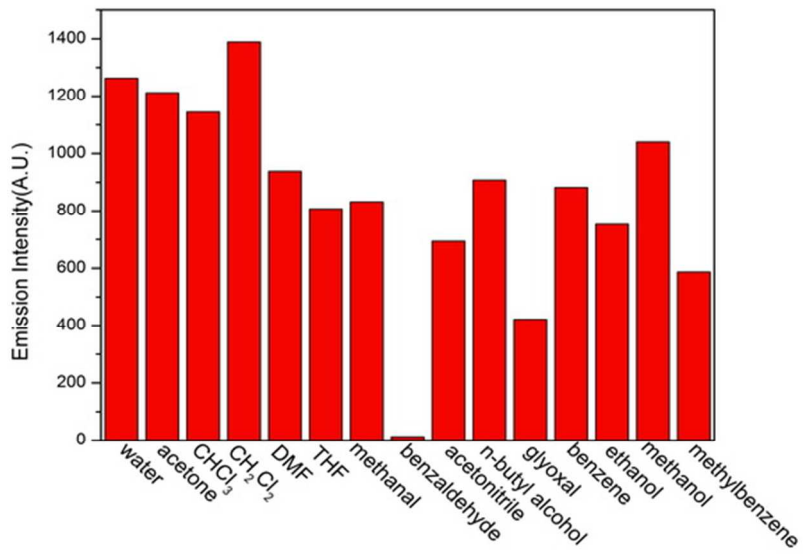

(a)

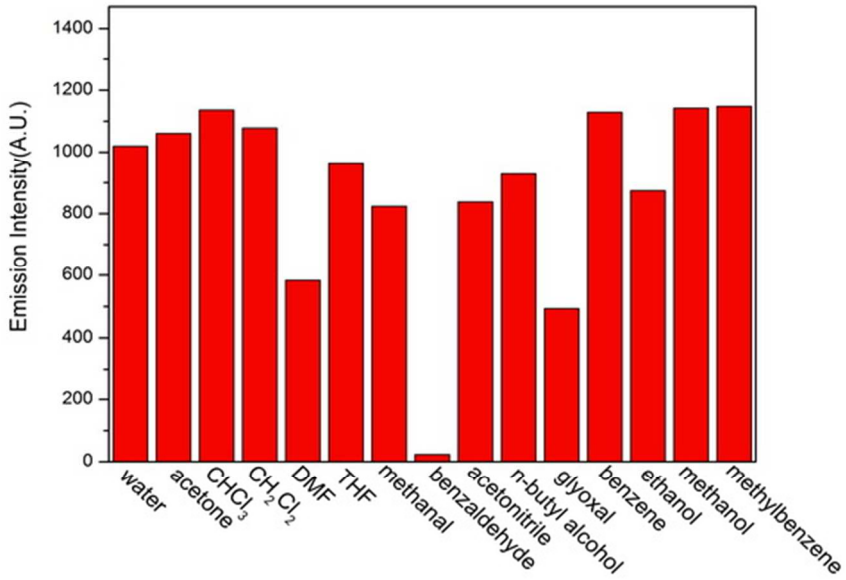

(b)

Figure 2. (a) Photoluminescence intensity of the $^5D_0 \rightarrow /^7F_2$ transition of **1** dispersed in different solvents, excited at 345 nm. (b) The $^5D_4 \rightarrow ^7F_5$ transition intensity of **2** dispersed in different solvents, excited at 332 nm.

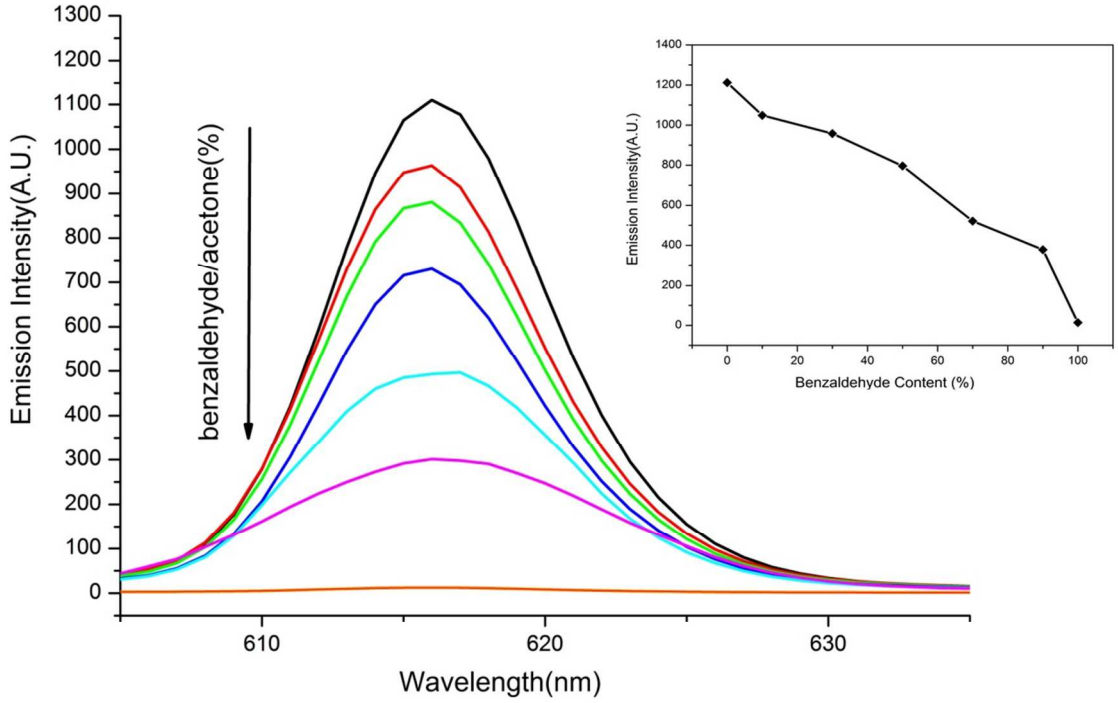

(a)

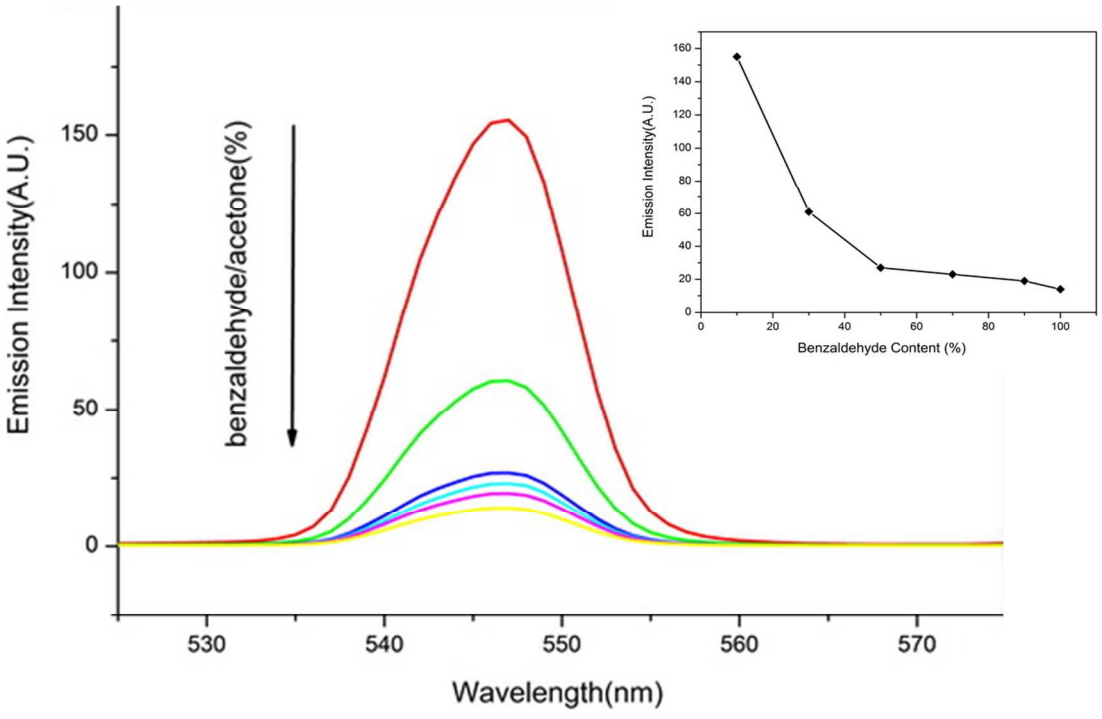

(b)

Figure 3. (a) Emissive response spectra of **1** for benzaldehyde in acetone solution with different benzaldehyde volume concentrations (insert is graph of the fluorescent intensity of **1,** acetone as a function of benzaldehyde content). (b) Emissive response spectra of **2** for benzaldehyde in acetone solution with different benzaldehyde volume concentrations (insert is graph of the fluorescent intensity of **2,** acetone as a function of benzaldehyde content).

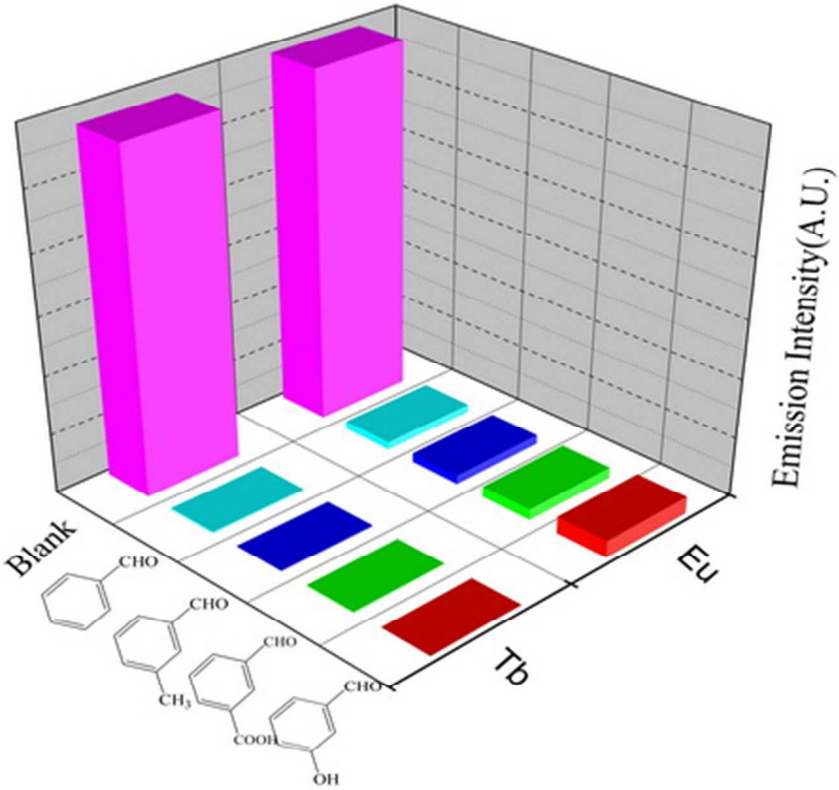

Figure 4. View of fluorescence intensity of **1** and **2** by four different aromatic analytes.

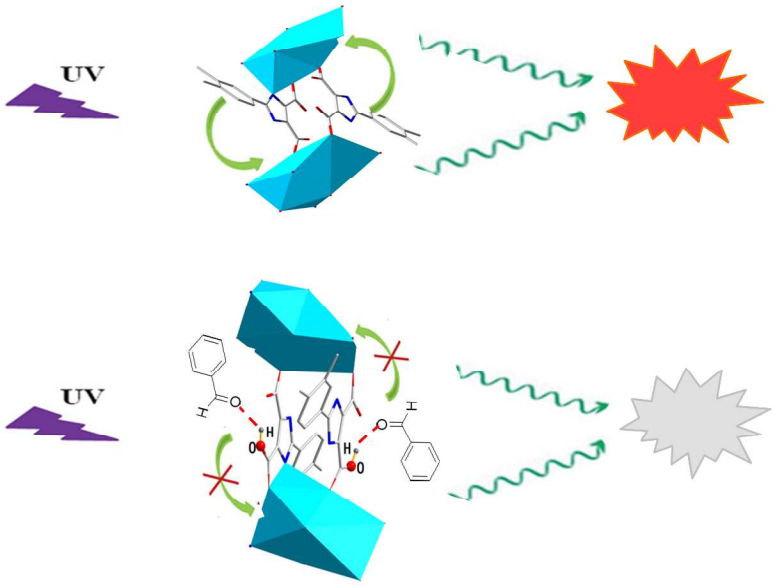

Figure 5. Luminescence quenching effect of **1** induced by benzaldehyde through a reduction of the antenna efficiency inside **1**, which may be due to the H-bonds interactions between benzaldehyde and the organic

ligands.

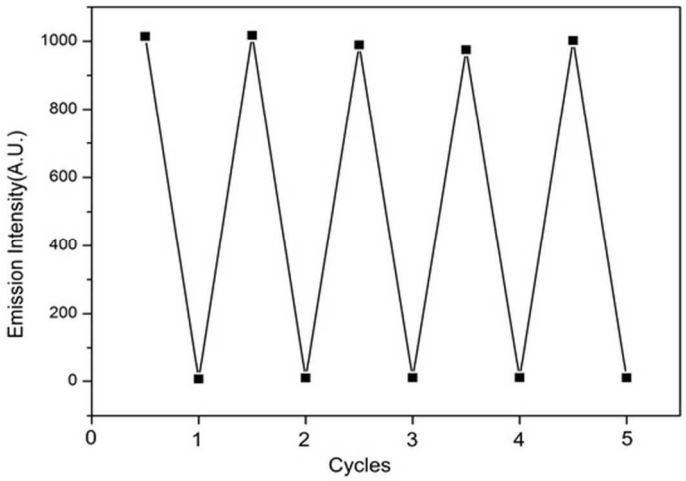

Figure 6. The quenching and recovery test of **1** in acetone solution. The up dots represent the initial luminescent intensity and the down dots represent the intensity upon addition of benzaldehyde.

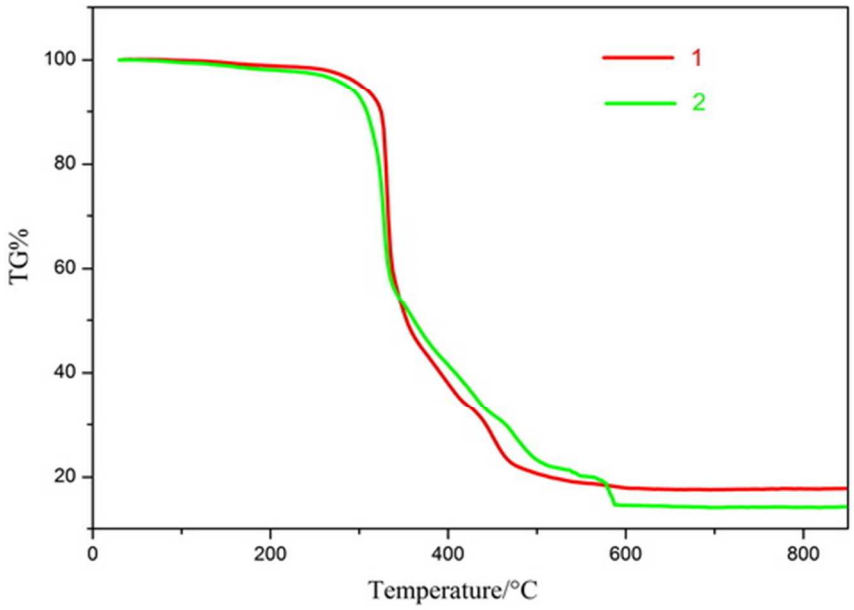

Figure 7. TG analysis profiles of compounds **1** and **2**.